



Influence of 2D and 3D Arrangements of Aramid Fibers on the Dart Drop Test of Epoxy Composites

Carlos Alberto Fernandes Marlet¹ , Thiago de Carvalho Silva^{1,2} , Mirabel Cerqueira Rezende^{1,*} 

1. Universidade Federal de São Paulo  – Instituto de Ciência e Tecnologia – Laboratório de Tecnologia de Polímeros e Biopolímeros — São José dos Campos/SP – Brasil **2.** Centro Federal de Educação Tecnológica Celso Suckow da Fonseca  – Coordenação de Engenharia Mecânica – Angra dos Reis/RJ – Brasil.

*Correspondence author: mirabel.rezende@unifesp.br

ABSTRACT

The use of continuous fibers reinforced polymeric composites has increased substantially in the last year's due to their high specific mechanical strength compared to other materials. Despite this property, this class of material is susceptible to low, medium, or high energy impacts, which can cause severe damage to composite laminates. One of the most serious damages is delamination, which can lead to partial or total rupture of the structure. In order to minimize this problem, several studies have been carried out in this area. In this context, this work aims to evaluate the influence of aramid reinforcement with bi-directional (2D) and tri-directional (3D) arrangements impregnated with two epoxy resins of different stiffness on the impact strength of composites submitted to the 340 J dart drop test. The impact results showed that the 2D composites had lower impact strength than the 3D ones, with the presence of perforations (when impregnated with the more rigid resin) and delaminations. Delaminations occurred regardless of the epoxy resin used in the impregnation. On the other hand, the 3D composites impregnated with the less rigid epoxy matrix absorbed more energy (3DF: 97.9%) with less deformation and no delamination compared to the 2D laminate (2DF: 96.1%) produced.

Keywords: Aramid/epoxy composites; 3D arrangement; Impact strength; Dart drop test.

INTRODUCTION

Industries are constantly improving their products, concerning physicochemical and mechanical properties, greater durability, and cost reduction. In this context, polymeric composite materials are included, resulting from the combination of two or more distinct components, forming a new material with superior mechanical properties to those of its individual constituents. This class of materials has been increasingly used in sectors that require higher specific properties of strength and stiffness and other advantages, such as lightweight, durability, and corrosion resistance, especially compared to metallic materials (Czél *et al.* 2015a; b; Kumar *et al.* 2006). In this case, the aeronautical, space, defense, automotive, energy, and sports industries stand out as areas that have made increasing use of polymer composites (Chawla 2019; Daniel and Ishai 2006; Gay 2015; Hagnell *et al.* 2016; Lan *et al.* 2015). Despite the advantages that this class of materials offers over conventional materials, its use can be limited by the presence of processing defects or damages that occur during its use, which can promote partial or total failure of the component.

Received: Feb 26, 2023 | **Accepted:** June 26, 2023

Section editor: José Atilio Fritz Rocco 

Peer Review History: Single Blind Peer Review.



This is an open access article distributed under the terms of the Creative Commons license.

Defects can be located on the outermost face, that is, on the surface, or within the composite structure. Surface defects can be present such as cracks, porosities, and geometric deformations, and are often detected by visual inspection, while internal defects in the structure require more sophisticated equipment, for example, ultrasound or computed tomography scans (Jones 1975; Karahan and Yildirim 2015).

In the case of composites obtained by lamination of reinforced layers, delamination is a possible critical internal defect, as it can promote partial or total separation between the laminated layers. And, its occurrence takes place in three stages. In the first, crack initiation occurs in the matrix. In the second, the crack propagation occurs through the matrix or through the reinforcement/matrix interface. Finally, in the third step, the layers are separated (Aiman *et al.* 2016). This type of defect can occur during the manufacture of the laminated composite, due to the displacement of layers or the presence of voids or pores, or even during the use of the component. In the latter situation, delamination can occur due to the impact of external loads, such as dropped tools, impacts with hail or gravel, collision with birds, or ballistic shocks (Dickinson *et al.* 1999).

There is no single way to classify the types of impacts. Vaidya (2011), for example, classifies the impacts as low-speed, those occurring below 10 m/s, intermediate speed (10 to 50 m/s), high-speed (50 to 1000 m/s), and hyper-speed for impacts that occur above 2000 m/s. Guimarães (2010) classifies impacts according to the damage caused, as high-speed impacts when the damage is easily identifiable and the material is completely perforated; medium-speed impacts those whose damage is not easily identifiable but promotes some deformation on the structure close to the impacted zone and, finally, low-speed impacts when the damaged area is not identifiable by visual inspection. Another impact classification criterion is related to the actuation time of load. In this case, the impacts are divided into two main categories: low-speed and high-speed impacts (Hodgkinson 2000; Sierakowski and Chaturvedi 1997). The first is characterized by having a larger damaged area and the response of the entire structure impacted, with the absorption of a large part of the impact energy. And the high-speed impact, on the other hand, causes more localized damage, with less affected region, with or without perforation (Ferreira 2007).

Among the cited classifications of impacts, a well-accepted classification considers high-speed impacts to be those that occur at speeds above 1000 m/s, which cause damage detected by visual inspection or ultrasound analyses. On the other hand, low-speed impacts involve speeds below 100 m/s that cause internal damage, mainly delamination, which is difficult to be detected (Costa 2009). When low-speed impacts occur with speeds below 10 m/s they are considered quasi-static. Impact damages are measured in terms of energy absorbed by the material and the depth of target deformation, caused by the impactor (Duell 2004). This type of test is usually performed through the dart drop test (or drop test) (Zhang and Richardson 2007).

Considering the susceptibility of laminated composites to the occurrence of delamination, the literature (Abrate 2011; Sastry *et al.* 2014; Sun *et al.* 2013) shows studies that use fiber tows to tie the layers in the direction of the thickness of the composite, sewing the layers together. Thus, promoting greater structural integrity, especially to impacts. Farley *et al.* (1992) observed that the presence of fiber tows in the thickness of laminates, that is, in the z-direction, increases the impact resistance of composites, due to greater energy absorption and the impact force dissipation. Cantwell and Morton (1991) showed that composites with some type of bonding between the layers have compression, bending, and impact strength properties increased by up to 20%. Already, Gerlach *et al.* (2012) described that the effect of carbon fiber in the z-direction considerably improved the delamination strength of composites lashed with two strands of carbon fiber, in bending tests.

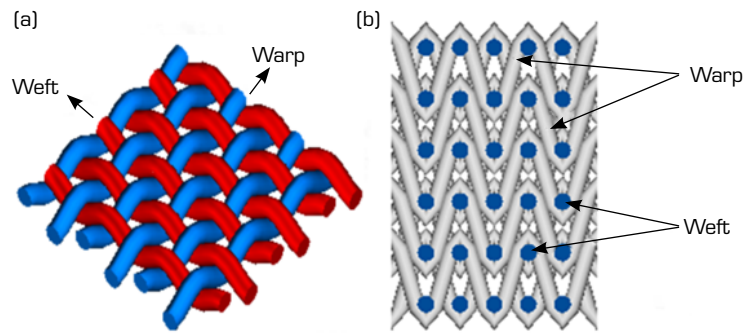
The literature also shows studies involving the impact tests of composites manufactured with different reinforcements (Barbosa *et al.* 2017; Karahan and Yildirim 2015; Thanomsilp and Hogg 2003). Among them, it is described that aramid composites presented less damaged regions than composites with Ultra High Molar Mass Polyethylene (UHMWPE) fibers and that the hybrid aramid and UHMWPE composites presented higher energy absorption compared to other configurations (Karahan and Yildirim 2015).

In summary, the consulted literature presented studies involving the tying of layers and the use of different fibers, but technical-scientific studies involving tri-directional (3D) reinforcements are not reported, aiming to improve the impact resistance and even to reduce the unwanted effect of delamination in laminated composites. In this context, this work contributes in this area with the study of the impact resistance of composites reinforced with aramid fibers arranged in bi-directional plain weave fabric (2D) and tri-directional reinforcements, impregnated with two different epoxy resins.

MATERIALS AND METHODS

Materials

This study used two samples of epoxy resins, the first is an Epocast code 50A1 (more rigid, code R) with curing agent Aradur 9816 (ratio 14% wt.), and the second resin is the epoxy GY260 modified with the agent DY3601 (less rigid, code F) with curing agent Aradur 2963 (ratio 25% wt.), both supplied by Huntsman International LLC. The two reinforcements used in this study were obtained with aramid fiber tows with 1000 filaments, 1570 deniers per tow, and 100 twists per meter, code Kevlar K29®, from DuPont-Brazil Ltda. The commercially available 2D fabric, code XPS103, had a plain weave-like arrangement (Fig. 1a). The reinforcement with the 3D arrangement was processed by the authors, as detailed in previous work (Marlet and Rezende 2021). This process was performed in a single step, that is, the 2D fabric manufacture (Fig. 1a) and the lashing in the z-direction were carried out in a unique step, using a machine specially developed for this purpose. The processed 3D-reinforcement using 6 layers of 2D plain weave fabric, intertwined with each other by warp filaments, is schematized in Fig. 1b.



Source: Adapted from Marlet and Rezende (2021).

Figure 1. Schematics of (a) 2D plain weave-style fabric and (b) the 3D reinforcement produced by the authors.

Table 1 shows the main characteristics of the 2D and 3D reinforcements used in this study.

Table 1. Characteristics of 2D and 3D reinforcements with aramid fiber.

Characteristics	3D	2D
Type of in-plane interlacing	Plain weave	Plain weave
Number of layers	6	1
Grammage (g/m ²)	1458.5 ± 14.8	221.0 ± 5.6
Thickness (mm)	3.7 ± 0.2	0.46 ± 0.07
Warp yarn title (denier)	1575.3 ± 18.0	1565.0 ± 20.0
Weft yarn title (denier)	1573.6 ± 19.4	1571.6 ± 19.4
Warp yarn density per layer (yarns/cm)	8.4 ± 0.5	6.6 ± 0.2
Weft yarn density per layer (yarns/cm)	6.2 ± 0.4	6.1 ± 0.4
Linear density of warp yarns (<i>crimp</i>) [%]	7.2 ± 2.6	0.94 ± 0.25
Linear density of weft yarns (<i>crimp</i>) [%]	1.5 ± 0.3	1.0 ± 0.2

Source: Elaborated by the authors using data from Marlet and Rezende (2021).

Preparation of composites

Table 2 details the conditions used in the preparation of the four different composite panels used in this study. The sample codes considered the type of reinforcement (2D or 3D) and the impregnating polymeric matrix used, i.e., R or F epoxy resins. The

panels with the 2D fabric were obtained by stacking 6 layers, which were impregnated with epoxy resins R (2DR family) and F (2DF family). The 3DR and 3DF panels were processed using the same polymeric matrices, but 1 layer of the 3D multilayer reinforcement, considering that this reinforcement is formed by 6 layers of 2D fabric tied in the third direction (Fig. 1b). The dimensions of the samples were 500 mm x 500 mm and the impregnation was carried out by hand layup process using an open mold with side frames, which ensured the dimensions of the composites at 500 mm x 500 mm. After impregnation, the mold was wrapped in a vacuum bag, with an adapted vacuum connection. The reinforcement:matrix ratio in all impregnations was 45:55%, by weight. After the impregnation, the mold involved by the vacuum bag was transferred to a laboratory oven, Palley model E-245, and the epoxy resin was cured at 140 °C, under a vacuum of 400 mmHg, for 3 h.

Table 2. Composite panels prepared.

Family	Reinforcement	Epoxy matrix	Number of layers
2DR	2D	Epocast 50A1 (R)	6
2DF	2D	GY260/DY3601 (F)	6
3DR	3D	Epocast 50A1 (R)	1
3DF	3D	GY260/DY3601 (F)	1

Source: Adapted from Marlet and Rezende (2021).

Characterization

The grammage of the composite panels was determined based on the NBR 10591 standard (ABNT 1988). For this, each sample was individually weighed on an analytical balance, Shimadzu model AUW220, with a precision of 0.1 mg. The mean values and the standard deviation were calculated based on Eq. 1, in triplicate.

$$\text{Grammage} \left(\frac{g}{m^2} \right) = \frac{Mc}{0.01 (m^2)} \quad (1)$$

where: Mc = dry weight of sample (g).

The matrix content of each composite family was determined according to ASTM D3171-22 standard (ASTM 2022), weighing each sample before the impregnation to obtain the weight of fiber and after the curing process to obtain the dry weight of the sample. Like this, the fiber content was calculated according to Eq. 2, in triplicate.

$$\text{Fiber content} (\%) = \frac{Mf \cdot dc}{Mc \cdot df} \cdot 100 \quad (2)$$

where: Mc = dry weight of sample (g); Mf = weight of fiber (g); dc = composite density (g/cm^3); df = fiber density (g/cm^3).

The density of composites was obtained by hydrostatic method, according to Eq. 3, in triplicate.

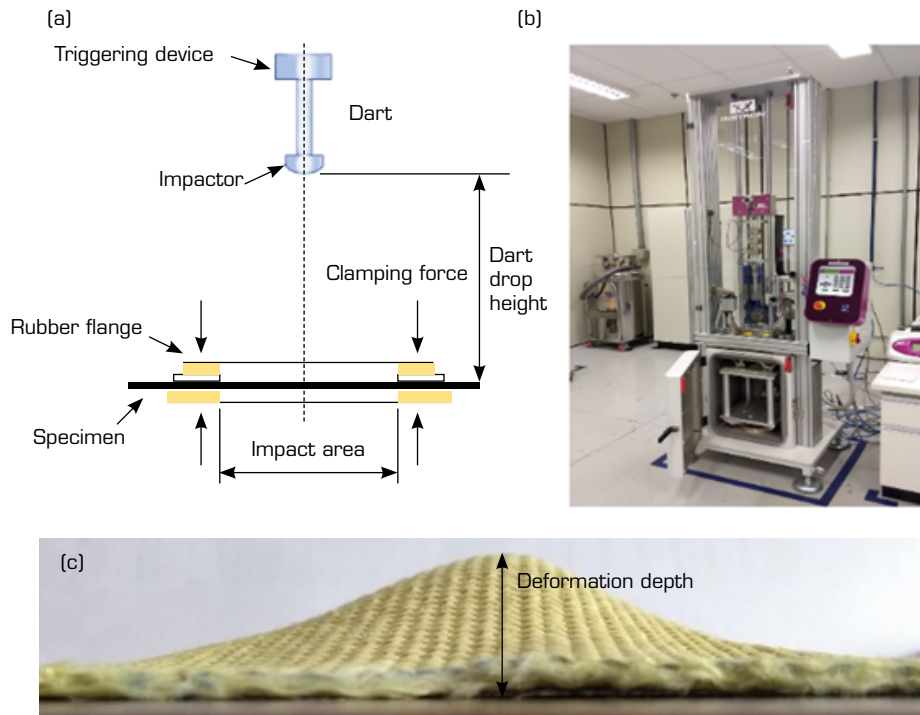
$$\text{Composite density} \left(\frac{g}{cm^3} \right) = \frac{Mc}{Mc - Mw} \times dw \quad (3)$$

where: Mc = dry weight of sample (g); Mw = weight of sample immersed in water (g); dw = water density (g/cm^3).

The dart drop tests were performed according to ASTM D7136/D7136M - 20 standard (ASTM 2020), using 5 specimens of each family, measuring 100 mm x 150 mm and a thickness of (3.74 ± 0.4) mm. The tests were carried out in a drop impact test machine Instron model CEAST 9340, at room temperature (25 ± 2) °C. A 32 kg dart was dropped from a height of 1.1 m. In this condition, the dart hits the specimen at a speed of 4.67 m/s, that is, with an impact energy of 340 J, which is the maximum energy available in the equipment used. The deformations and the depth of the impacted area on the specimen were measured using a caliper. Deformation depth was measured from the highest point of deformation to the surface where the sample was positioned, as shown in Fig. 2c. Figure 2a illustrates the dart test setup and Fig. 2b the testing machine used. The absorbed energy is recorded by the data acquisition system and calculated through Eq. 4, presented in the ASTM D7136/D7136 - 20 standard (ASTM 2020).

$$E_a(t) = \frac{m(v_i^2 - v(t)^2)}{2} + mg\delta(t) \quad (4)$$

where: E_a = absorbed energy at time t (J); v_i = impact velocity (m/s); v = impactor velocity at time t (m/s); m = mass of impactor (kg); g = acceleration due to gravity (9.81 m/s²); δ = impactor displacement at time t (m).



Source: Adapted from Marlet and Rezende (2021).

Figure 2. (a) Dart impact testing setup; (b) dart drop impact test machine (Instron model CEAST 9340); (c) measure of deformation depth.

The samples were analyzed by optical stereoscopy, using a portable equipment, Instrutherm pen type, model MP-150.

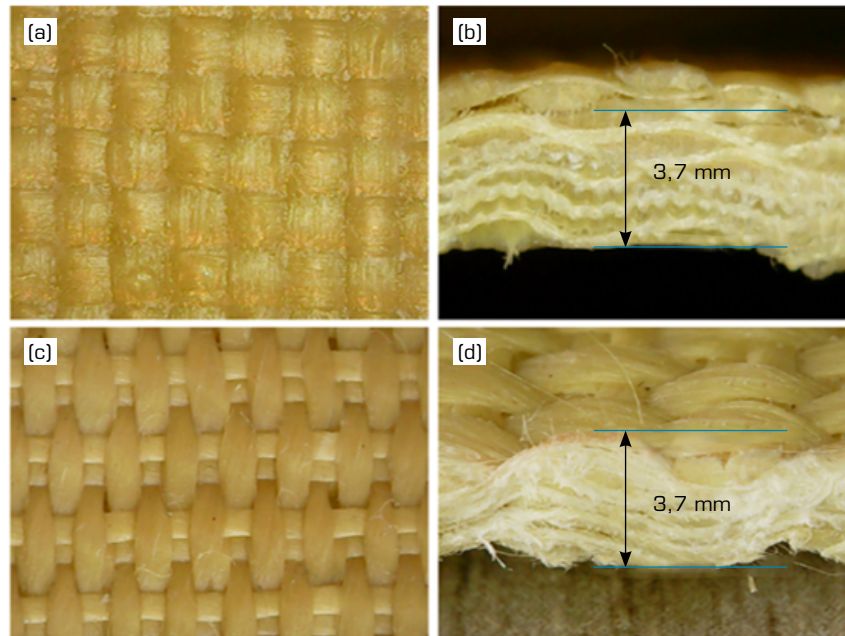
Ultrasound inspection of the panels was performed using the pulse-echo technique, in a Kratkramer USM 36 equipment, model V202, with a 5 MHz transducer.

RESULTS AND DISCUSSION

Figure 3 shows representative images of the panels processed with the 2D and 3D reinforcements impregnated with the epoxy resin F. Similar images were obtained for the panels impregnated with epoxy resin R. Analysis of these images shows that the panels were processed successfully. Visual inspection does not show the presence of defects and regions rich in resin or fibers. Figure 3c and d shows the more complex arrangement of the aramid tows in the 3D configuration.

Table 3 shows the values of grammage, density, and contents of fiber and polymeric matrix of all families of the studied composites. The analysis of these results shows that the DY3601 agent present in the epoxy resin F promoted the reduction of the grammage values of the composites 2DF and 3DF (2153.0 ± 12.7 g/m² and 2196.9 ± 33.6 g/m², respectively, in relation to the 2DR and 3DR composites, impregnated with the epoxy resin R (2787.7 ± 50.1 g/m² and 2832.0 ± 46.7 g/m², respectively). Similar behavior is observed for the density values of these composites, that is, the density of samples impregnated with the epoxy resin F decreased. On the other hand, the fiber content increased. The correlation of these data shows that the addition of the DY3601 agent decreased the viscosity of the epoxy matrix, which probably improved the impregnation of the reinforcement. However, during the curing process under vacuum, the F resin was more easily extracted from the reinforcement, enriching the

final composite in fibers and voids, and consequently, decreasing the grammage and density values. Regarding the fiber content in the composites, the 2D-based samples show a slight increase. This behavior can be attributed to the better densification of the plain weave fabric layers since, in the 3D arrangement, the lashing of the third direction by the warp fiber tows induces a greater presence of voids in the reinforcement.



Source: Elaborated by the authors.

Figure 3. Top and cross-section views of the 2D (a, b) and 3D (c, d) composite panels.

Table 3. Grammage, density, fiber and resin contents of composites.

Family	Grammage (g/m ²)	Composite density (g/cm ³)	Fiber content (%)	Matrix content (%)
2DR	2787.7 ± 50.1	1.08 ± 0.01	47.6 ± 1.2	52.4 ± 0.6
2DF	2153.0 ± 12.7	0.88 ± 0.02	61.6 ± 1.6	38.4 ± 1.0
3DR	2832.0 ± 46.7	1.07 ± 0.01	46.9 ± 0.5	53.1 ± 1.1
3DF	2196.9 ± 33.6	0.80 ± 0.01	60.5 ± 0.6	39.5 ± 0.8

Source: Elaborated by the authors using data from Marlet and Rezende (2021)

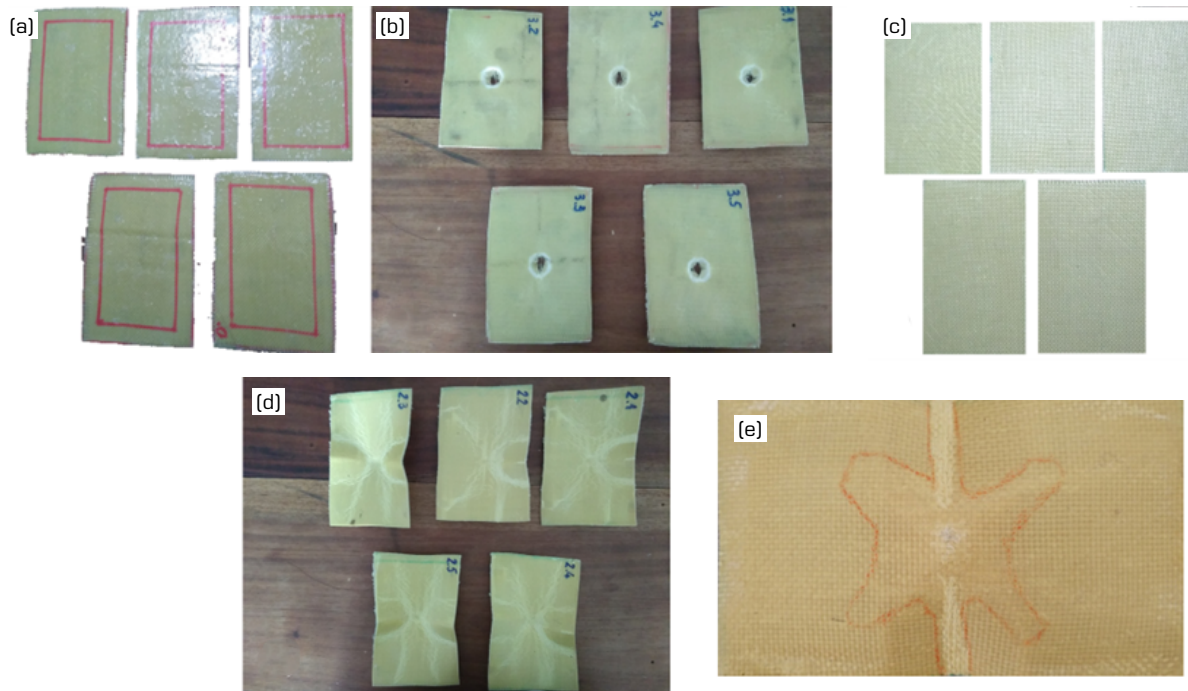
Figures 4 and 5 show specimens processed with 2D and 3D reinforcements, respectively, before and after the impact tests, impregnated with the epoxy resins R and F. Figure 4a and c shows, respectively, the specimens of the 2DR and 2DF families before the impact and Fig. 4b and d the samples after the impact tests. The comparative analysis of these samples shows that the specimens prepared with the 2D reinforcement impregnated with the more rigid resin (R) were completely perforated, while those impregnated with the less rigid epoxy resin (F) were deformed, but without perforation. In this case, the mean value of depth of deformation for the 2DR specimens was 12.4 mm with an absorbed energy value of (255.7 ± 46.1) J/m, that is, 75.2% of the impact energy was absorbed by the 2DR composite (Table 4). This absorbed energy value is lower than the mean value obtained for 2DF laminates (326.7 J/m) (96.1%), whose penetration depth was (12.8 ± 0.1) mm, without perforation. In the case of the 2DR family, part of the energy was dissipated in the perforation process of the sample. On the other hand, most of the impact energy was absorbed by the 2DF family, with the deformation of the sample, without perforation. This behavior is due to the less rigid characteristic of the epoxy resin F used in the impregnation of this composite. According to Syed Abdullah (2021), the elastic deformation capacity of composites processed with thermoplastic or elastomeric matrices is an important factor to improve the resistance to impact penetration. Table 4 summarizes these results.

Table 4. Results of the dart drop impact tests with 340 J.

Family	Deformation depth (mm)	Absorbed energy (J/m)	Absorbed energy (%)	Perforation
2DR	12.4 ± 1.4	255.7 ± 46.1	75.2	FP
2DF	12.8 ± 0.1	326.7 ± 0.9	96.1	NP
3DR	16.3 ± 0.7	187.2 ± 21.7	55.1	FP
3DF	14.0 ± 0.8	332.8 ± 3.3	97.9	NP

FP = full perforation e NP = no perforation. Source: Elaborated by the authors.

Figure 4e shows the delaminated area of the 2DF sample after impact (region marked by the red line) obtained by ultrasound inspection. Although this sample is not showing perforation, this image shows extensive delamination that compromised the quality of the composite. The samples with perforation were not inspected by ultrasound and neither were the composites with 3D reinforcement, as the surface roughness did not allow the analysis to be carried out.

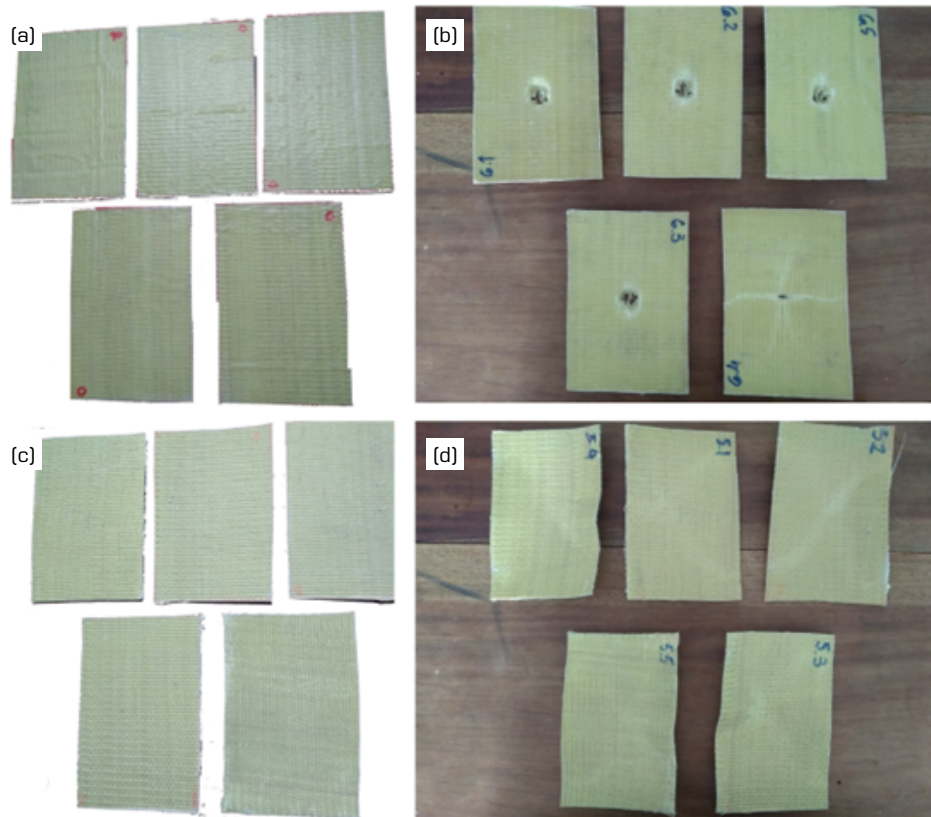


Source: Elaborated by the authors.

Figure 4. Top view from 2DR and 2DF composites before (a, c) and after (b, d) the dart drop impact test and delaminated region of the 2DF obtained by ultrasound inspection (e).

Figure 5a and c shows, respectively, the specimens processed with the tri-directional reinforcement (3DR and 3DF) before impact, and Fig. 5b and d show the specimens after the dart drop tests. As can be seen in Fig. 5b, the 3DR specimens were perforated, while the composites with the less rigid resin (3DF) were only deformed, without perforation. The mean deformation value of the 3DR samples was 16.3 mm, measured with a caliper, with absorbed energy of 187.2 J/m (55.1%). 3DF composites, on the other hand, show deformation with a depth of 14.0 mm and more absorbed energy, that is, 332.8 J/m (97.9%) (Table 4).

Table 4 shows that all laminates impregnated with the less rigid resin (2DF and 3DF) showed the highest energy absorption values, respectively 96.1% and 97.9%, without perforation of the specimens. On the other hand, the laminates impregnated with the most rigid resin (2DR and 3DR) present, respectively 75.2% and 55.1% of energy absorption, during the dart drop impact tests. The lower energy absorption presented by the 3DR composite is attributed to the higher matrix content in this sample (53.3%, as shown in Table 3).



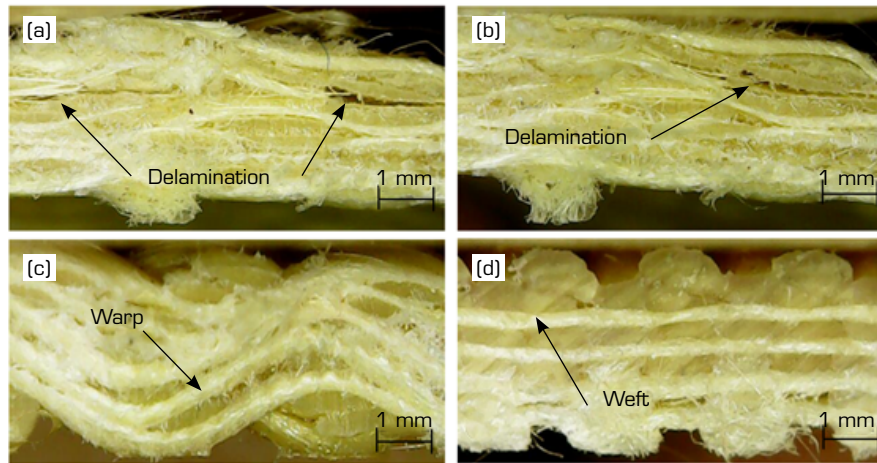
Source: Elaborated by the authors.

Figure 5. Top view from specimens of the 3DR and 3DF composites before (a, c) and after (b, d) the dart drop impact test.

Regarding the deformation depth, the composites processed with the 3D reinforcement, regardless of the resin used in the impregnation (R or F), show higher values (16.3 mm and 14.0 mm) than those observed for the 2D fabric (12.4 mm and 12.8 mm). This behavior is attributed to the arrangement of fiber cables in the 3D reinforcement structure, that has a configuration in which the warp tows, responsible for tying between the layers, have a higher linear density (crimp) (7.2%), as shown in Table 1. Therefore, less tension than the 2D fabric warp tows (0.94%). The higher linear density of the aramid tows of warp in the 3D reinforcement allows greater deformation in the cross-section of the specimen (in depth) and greater absorption of impact energy. In laminates with 2D fabric, impregnated with both epoxy matrices (R and F), the warp threads have a lower linear density (crimp) (Table 1) and, therefore, less deformation during impact, causing the break of aramid tow, with the perforation of the specimens and, consequently, less energy absorption.

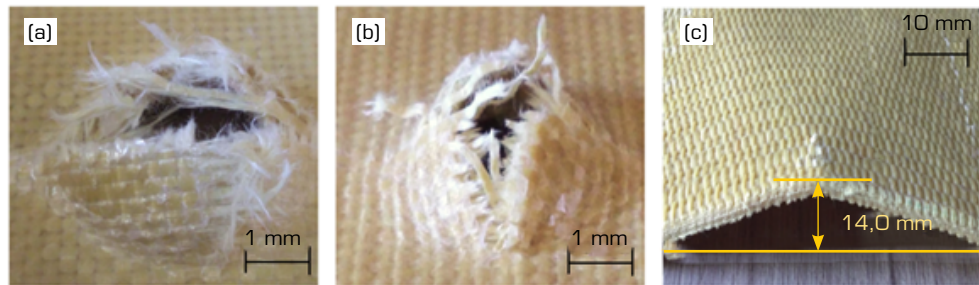
Figure 6a and b shows the cross-section views of the impacted region of the 2DF family in the warp (Fig. 6a) and weft (Fig. 6b) directions. Although this family does not show perforation in the impact tests, the analysis of the cross-sections shows delaminations in both directions of the laminate (black arrows). On the other hand, the cross-section views of the 3DF composites do not show delaminations, in both directions, that is, in the warp (Fig. 6c) and weft (Fig. 6d) directions. This figure also shows the warp tow used to tie the layers (Fig. 6c) and the weft tow without waviness (Fig. 6d).

Figure 7 shows, respectively, the 2DR (Fig. 7a) and 3DR (Fig. 7b) samples processed with the more rigid epoxy matrix (R). These samples show the perforation caused by the dart drop, with broken aramid tows and delaminations. Figure 7a shows a typical plain weave arrangement of the aramid tows, with pulled fibers, and Fig. 7b shows the more complex arrangement of the tows in the 3D structure. Although Fig. 7b shows a perforation, compared to Fig. 7a, this figure shows less pulled fibers, probably due to fiber tying. Figure 7c is representative of 3D reinforcement impregnated with resin F, without perforation and significant delamination, only panel deformation.



Source: Elaborated by the authors.

Figure 6. Cross-section of the impacted region of the 2DF composite in (a) warp and (b) weft directions, and 3DF composite in (c) warp and (d) weft directions.



Source: Elaborated by the authors.

Figure 7. Composites 2DR (a), 3DR (b), and 3DF (c) composites after the drop test.

CONCLUSIONS

This study shows the preparation of polymeric composites obtained by the authors using 3D reinforcement with aramid fiber tows. The 3D reinforcement was obtained in a single step, involving the 2D fabric manufacture and the simultaneous lashing in the z-direction, using a machine specially developed for this purpose. The results obtained in this study showed that the composite processed with the 3D reinforcement and impregnated with the less rigid epoxy resin presented the highest impact resistance in the dart drop test at a speed of 4.67 m/s, compared to the 2D composites. The 3D composite impregnated with the less rigid matrix absorbed about 97.9% ((332.8 ± 3.3) J/m) of the impact energy, without delaminations and perforation. On the other hand, composites with 2D and 3D reinforcements impregnated with the more rigid epoxy resin absorbed less energy, 75.2% and 55.1%, respectively, and all were perforated, regardless of the reinforcement used. In summary, this study shows that the 3D composite presented more advantages, noting that there was no evidence of delamination, regardless of the epoxy resin used in the impregnation. Furthermore, when the 3D composite was impregnated with the less rigid polymer matrix, no perforation of the sample occurred. This behavior shows the potential of using 3D reinforcement in different applications subject to medium energy impacts (340 J).

CONFLICT OF INTEREST

Nothing to declare.

AUTHOR CONTRIBUTIONS

Conceptualization: Marlet CAF and Rezende MC; **Formal analysis:** Marlet CAF and Rezende MC; **Acquisition of funding:** Marlet CAF and Rezende MC; **Research:** Marlet CAF and Rezende MC; **Methodology:** Marlet CAF and Rezende MC; **Project administration:** Marlet CAF and Rezende MC; **Software:** Not applicable; **Supervision:** Rezende MC; **Visualization:** Rezende MC; **Writing - Preparation of original draft:** Marlet CAF; Silva TC and Rezende MC; **Writing – Proofreading and editing:** Marlet CAF; Silva TC and Rezende MC.

DATA AVAILABILITY STATEMENT

The data will be available upon request.

FUNDING

Coordenação de Aperfeiçoamento de Pessoal de Nível Superior

[<https://doi.org/10.13039/501100002322>]

Finance Code 001

Fundação de Amparo à Pesquisa do Estado de São Paulo.

[<https://doi.org/10.13039/501100001807>]

Grant No: 2015/50065-7

Conselho Nacional de Desenvolvimento Científico e Tecnológico

[<https://doi.org/10.13039/501100003593>]

Grant No: 305123/2018-1

ACKNOWLEDGEMENTS

The authors also thank TECPLAS Indústria e Comércio Ltda/Brazil for providing its infrastructure for the manufacture of the 3D reinforcement and the preparation of specimens, and also the Light Structures Laboratory (LEL) of the Instituto de Pesquisas Tecnológicas (IPT)/Brazil for supporting the impact tests.

REFERENCES

[ABNT] Associação Brasileira de Normas Técnicas (1988) NBR10591: Materiais têxteis – Determinação Da Gramatura de Tecidos. Rio de Janeiro: ABNT.

Abrate S (2011) Impact engineering of composite structures. Vienna: Springer. <https://doi.org/10.1007/978-3-7091-0523-8>

Aiman DPC, Yahya MF, Salleh J (2016) Impact properties of 2D and 3D woven composites: a review. AIP Conf Proc 1774:020002. <https://doi.org/10.1063/1.4965050>

- [ASTM] American Society for Testing and Materials (2020) ASTM D7136/D7136M-20: Standard Test Method for Measuring the Damage Resistance of a Fiber-Reinforced Polymer Matrix Composite to a Drop-Weight Impact Event. West Conshohocken: ASTM.
- [ASTM] American Society for Testing and Materials (2022) D3171-22: Standard Test Methods for Constituent Content of Composite Materials. West Conshohocken: ASTM.
- Barbosa LA, Dreger AA, Schneider EL, Morisso FDP, Santana RM (2017) Polietileno de baixa densidade - PEBD: mercado, produção, principais propriedades e aplicações. *Espacios* 38(17):10.
- Cantwell WJ, Morton J (1991) The impact resistance of composite materials – a review. *Composit* 22(5):347-362. [https://doi.org/10.1016/0010-4361\(91\)90549-V](https://doi.org/10.1016/0010-4361(91)90549-V)
- Chawla KK (2019) *Composite Materials: Science and Engineering*. Cham: Springer. <https://doi.org/10.1007/978-3-030-28983-6>
- Costa IEG (2009) Estudo do comportamento de estruturas sandwich com núcleos de cortiça para pás de turbinas eólicas (master's thesis). Porto: Universidade Porto. In Portuguese.
- Czél G, Pimenta S, Wisnom MR, Robinson P (2015a) Demonstration of pseudo-ductility in unidirectional discontinuous carbon fibre/epoxy prepreg composites. *Compos Sci Technol* 106:110-119. <https://doi.org/10.1016/j.compscitech.2014.10.022>
- Czél G, Jalalvand M, Wisnom MR (2015b) Demonstration of pseudo-ductility in unidirectional hybrid composites made of discontinuous carbon/epoxy and continuous glass/epoxy plies. *Compos Part A Appl Sci Manuf* 72:75-84. <https://doi.org/10.1016/j.compositesa.2015.01.019>
- Daniel IM, Ishai O (2006) *Engineering Mechanics of composite materials*. New York: Oxford University Press.
- Dickinson L, Farley GL, Hinders MK (1999) Prediction of Effective Three-Dimensional Elastic Constants of Translaminar Reinforced Composites. *J Compos Mater* 33(11):1002-1029. <https://doi.org/10.1177/002199839903301104>
- Duell JM (2004) Impact testing of advanced composites. In: Kessler MR, editor. *Advanced Topics in Characterization of Composites*. Canada: Trafford Publishing. p. 97-112.
- Farley GL, Smith BT, Maiden J (1992) Compression Response of Thick Layer Composite Laminates with Through-Thickness Reinforcement. *J Reinf Plast Compos* 11(7):787-810. <https://doi.org/10.1177/073168449201100705>
- Ferreira LMS (2007) Avaliação do dano em compósitos laminados devido a impactos de baixa velocidade (doctoral dissertation). Coimbra: Universidade de Coimbra. In Portuguese.
- Gay D (2015) *Composite materials: design and applications*. Boca Raton: CRC Press.
- Gerlach R, Siviour CR, Wiegand J, Petrinic N (2012) In-plane and through-thickness properties, failure modes, damage and delamination in 3D woven carbon fibre composites subjected to impact loading. *Compos Sci Technol* 72(3):397-411. <https://doi.org/10.1016/j.compscitech.2011.11.032>
- Guimarães LGS (2010) Compressão de placas compósitas após submetidas a impacto de baixa velocidade (doctoral dissertation). Coimbra: Universidade de Coimbra. In Portuguese.
- Hagnell MK, Langbeck B, Åkermo M (2016) Cost efficiency, integration and assembly of a generic composite aeronautical wing box. *Compos Struct* 152:1014-1023. <https://doi.org/10.1016/j.compstruct.2016.06.032>
- Hodgkinson JM (2000) *Mechanical Testing of Advanced Fibre Composites*. Cambridge: Woodhead Publishing Limited. <https://doi.org/10.1533/9781855738911>

- Jones RM (1975) *Mechanics of composite materials*. Washington: Scripta Book Company.
- Karahan M, Yildirim K (2015) Low Velocity Impact Behaviour of Aramid and UHMWPE Composites. *Fibres Text East Eur* 23;3(111):97-105. <https://doi.org/10.5604/12303666.1152522>
- Kumar SB, Sridhar I, Sivashanker S, Osiyemi SO, Bag A (2006) Tensile failure of adhesively bonded CFRP composite scarf joints. *Mater Sci Eng B* 132(1-2):113-120. <https://doi.org/10.1016/j.mseb.2006.02.046>
- Lan M, Cartié D, Davies P, Baley C (2015) Microstructure and tensile properties of carbon-epoxy laminates produced by automated fibre placement: Influence of a caul plate on the effects of gap and overlap embedded defects. *Compos Part A Appl Sci Manuf* 78:124-134. <https://doi.org/10.1016/j.compositesa.2015.07.023>
- Marlet CAF, Rezende MC (2021) Obtenção e caracterização de tecido multicamadas tridimensional de fibra de aramida visando aplicação em blindagem balística. *Matéria (Rio J.)* 26(1):e12947. <https://doi.org/10.1590/s1517-707620210001.1247>
- Sastry YBS, Budarapu PR, Krishna Y, Devaraj S (2014) Studies on ballistic impact of the composite panels. *Theor Appl Fract Mech* 72:2-12. <https://doi.org/10.1016/j.tafmec.2014.07.010>
- Sierakowski RL, Chaturvedi SK (1997) *Dynamic Loading and Characterization of Fiber-Reinforced Composites*. Canada: John Wiley & Sons.
- Sun D, Chen X, Mrango M (2013) Investigating ballistic impact on fabric targets with gripping yarns. *Fibers Polym* 14(7):1184-1189. <https://doi.org/10.1007/s12221-013-1184-2>
- Syed Abdullah SIB (2021) Low Velocity Impact Testing on Laminated Composites. In: Hameed Sultan MT, Shah AUM, Saba N, editors. *Impact studies of composite materials*. Singapore: Springer. p. 1-17. https://doi.org/10.1007/978-981-16-1323-4_1
- Thanomsilp C, Hogg PJ (2003) Penetration impact resistance of hybrid composites based on commingled yarn fabrics. *Compos Sci Technol* 63(3-4):467-482. [https://doi.org/10.1016/S0266-3538\(02\)00233-6](https://doi.org/10.1016/S0266-3538(02)00233-6)
- Vaidya UK (2011) Impact Response of Laminated and Sandwich Composites. In: Abrate S, editor. *Impact Engineering of Composite Structures*. CISM International Centre for Mechanical Sciences. Vienna: Springer. p. 97-191. https://doi.org/10.1007/978-3-7091-0523-8_4
- Zhang ZY, Richardson MOW (2007) Low velocity impact induced damage evaluation and its effect on the residual flexural properties of pultruded GRP composites. *Compos Struct* 81(2):195-201. <https://doi.org/10.1016/j.compstruct.2006.08.019>